

Measurement of branching fractions for D meson decaying into ϕ meson and a pseudoscalar meson

BESIII Collaboration

M. Ablikim^a, M.N. Achasov^{j,4}, P. Adlarson^{bn}, S. Ahmed^o, M. Albrecht^d, M. Alekseev^{bk,bm}, A. Amoroso^{bk,bm}, F.F. An^a, Q. An^{bh,as}, Y. Bai^{ar}, O. Bakina^{ac}, R. Baldini Ferroli^w, I. Balossino^y, Y. Ban^{ak,12}, K. Begzsuren^{aa}, J.V. Bennett^e, N. Berger^{ab}, M. Bertani^w, D. Bettoni^y, F. Bianchi^{bk,bm}, J. Biernat^{bn}, J. Bloms^{be}, I. Boyko^{ac}, R.A. Briere^e, H. Cai^{bo}, X. Cai^{a,as}, A. Calcaterra^w, G.F. Cao^{a,az}, N. Cao^{a,az}, S.A. Cetin^{aw}, J. Chai^{bm}, J.F. Chang^{a,as}, W.L. Chang^{a,az}, G. Chelkov^{ac,2,3}, D.Y. Chen^f, G. Chen^a, H.S. Chen^{a,az}, J.C. Chen^a, M.L. Chen^{a,as}, S.J. Chen^{ai}, Y.B. Chen^{a,as}, W. Cheng^{bm}, G. Cibinetto^y, F. Cossio^{bm}, X.F. Cui^{aj}, H.L. Dai^{a,as}, J.P. Dai^{an,8}, X.C. Dai^{a,az}, A. Dbeyssi^o, D. Dedovich^{ac}, Z.Y. Deng^a, A. Denig^{ab}, I. Denysenko^{ac}, M. Destefanis^{bk,bm}, F. De Mori^{bk,bm}, Y. Ding^{ag}, C. Dong^{aj}, J. Dong^{a,as}, L.Y. Dong^{a,az}, M.Y. Dong^{a,as,az}, Z.L. Dou^{ai}, S.X. Du^{br}, J.Z. Fan^{au}, J. Fang^{a,as}, S.S. Fang^{a,az}, Y. Fang^a, R. Farinelli^{y,z}, L. Fava^{bl,bm}, F. Feldbauer^d, G. Felici^w, C.Q. Feng^{bh,as}, M. Fritsch^d, C.D. Fu^a, Y. Fu^a, Q. Gao^a, X.L. Gao^{bh,as}, Y. Gao^{bi}, Y. Gao^{au}, Y.G. Gao^f, Z. Gao^{bh,as}, B. Garillon^{ab}, I. Garzia^y, E.M. Gersabeck^{bc}, A. Gilman^{bd}, K. Goetzen^k, L. Gong^{aj}, W.X. Gong^{a,as}, W. Gradl^{ab}, M. Greco^{bk,bm}, L.M. Gu^{ai}, M.H. Gu^{a,as}, S. Gu^b, Y.T. Gu^m, A.Q. Guo^v, L.B. Guo^{ah}, R.P. Guo^{al}, Y.P. Guo^{ab}, A. Guskov^{ac}, S. Han^{bo}, X.Q. Hao^p, F.A. Harris^{ba}, K.L. He^{a,az}, F.H. Heinsius^d, T. Held^d, Y.K. Heng^{a,as,az}, M. Himmelreich^{k,7}, Y.R. Hou^{az,*}, Z.L. Hou^a, H.M. Hu^{a,az}, J.F. Hu^{an,8}, T. Hu^{a,as,az}, Y. Hu^a, G.S. Huang^{bh,as}, J.S. Huang^p, X.T. Huang^{am}, X.Z. Huang^{ai}, N. Huesken^{be}, T. Hussain^{bj}, W. Ikegami Andersson^{bn}, W. Imoehl^v, M. Irshad^{bh,as}, Q. Ji^a, Q.P. Ji^p, X.B. Ji^{a,az}, X.L. Ji^{a,as}, H.L. Jiang^{am}, X.S. Jiang^{a,as,az}, X.Y. Jiang^{aj}, J.B. Jiao^{am}, Z. Jiao^r, D.P. Jin^{a,as,az}, S. Jin^{ai}, Y. Jin^{bb}, T. Johansson^{bn}, N. Kalantar-Nayestanaki^{ae}, X.S. Kang^{ag}, R. Kappert^{ae}, M. Kavatsyuk^{ae}, B.C. Ke^a, I.K. Keshk^d, A. Khoukaz^{be}, P. Kiese^{ab}, R. Kiuchi^a, R. Kliemt^k, L. Koch^{ad}, O.B. Kolcu^{aw,6}, B. Kopf^d, M. Kuemmel^d, M. Kuessner^d, A. Kupsc^{bn}, M. Kurth^a, M.G. Kurth^{a,az}, W. Kühn^{ad}, J.S. Lange^{ad}, P. Larin^o, L. Lavezzi^{bm}, H. Leithoff^{ab}, T. Lenz^{ab}, C. Li^{bn}, Cheng Li^{bh,as}, D.M. Li^{br}, F. Li^{a,as}, F.Y. Li^{ak,12}, G. Li^a, H.B. Li^{a,az}, H.J. Li^{i,10}, J.C. Li^a, J.W. Li^{aq}, Ke Li^a, L.K. Li^a, Lei Li^c, P.L. Li^{bh,as}, P.R. Li^{af}, Q.Y. Li^{am}, W.D. Li^{a,az}, W.G. Li^a, X.H. Li^{bh,as}, X.L. Li^{am}, X.N. Li^{a,as}, Z.B. Li^{at}, Z.Y. Li^{at}, H. Liang^{a,az}, H. Liang^{bh,as}, Y.F. Liang^{ap}, Y.T. Liang^{ad}, G.R. Liao^l, L.Z. Liao^{a,az}, J. Libby^u, C.X. Lin^{at,*}, D.X. Lin^o, Y.J. Lin^m, B. Liu^{an,8}, B.J. Liu^a, C.X. Liu^a, D. Liu^{bh,as}, D.Y. Liu^{an,8}, F.H. Liu^{ao}, Fang Liu^a, Feng Liu^f, H.B. Liu^m, H.M. Liu^{a,az}, Huanhuan Liu^a, Huihui Liu^q, J.B. Liu^{bh,as}, J.Y. Liu^{a,az}, K. Liu^a, K.Y. Liu^{ag}, Ke Liu^f, L.Y. Liu^m, Q. Liu^{az}, S.B. Liu^{bh,as}, T. Liu^{a,az}, X. Liu^{af}, X.Y. Liu^{a,az}, Y.B. Liu^{aj}, Z.A. Liu^{a,as,az}, Zhigang Liu^{am}, Y.F. Long^{ak,12}, X.C. Lou^{a,as,az}, H.J. Lu^r, J.D. Lu^{a,az}, J.G. Lu^{a,as}, Y. Lu^a, Y.P. Lu^{a,as}, C.L. Luo^{ah}, M.X. Luo^{bq}, P.W. Luo^{at}, T. Luo^{i,10}, X.L. Luo^{a,as}, S. Lusso^{bm}, X.R. Lyu^{az}, F.C. Ma^{ag}, H.L. Ma^a, L.L. Ma^{am}, M.M. Ma^{a,az}, Q.M. Ma^a, X.N. Ma^{aj}, X.X. Ma^{a,az}, X.Y. Ma^{a,as}, Y.M. Ma^{am}, F.E. Maas^o, M. Maggiora^{bk,bm}, S. Maldaner^{ab}, S. Malde^{bf}, Q.A. Malik^{bj}, A. Mangoni^x, Y.J. Mao^{ak,12}, Z.P. Mao^a, S. Marcello^{bk,bm}, Z.X. Meng^{bb}

J.G. Messchendorp^{ae}, G. Mezzadri^y, J. Min^{a,as}, T.J. Min^{ai}, R.E. Mitchell^v, X.H. Mo^{a,as,az}, Y.J. Mo^f, C. Morales Morales^o, N.Yu. Muchnoi^{j,4}, H. Muramatsu^{bd}, A. Mustafa^d, S. Nakhoul^{k,7}, Y. Nefedov^{ac}, F. Nerling^{k,7}, I.B. Nikolaev^{j,4}, Z. Ning^{a,as}, S. Nisar^{h,11}, S.L. Niu^{a,as}, S.L. Olsen^{az}, Q. Ouyang^{a,as,az}, S. Pacetti^x, Y. Pan^{bh,as}, M. Papenbrock^{bn}, P. Patteri^w, M. Pelizaeus^d, H.P. Peng^{bh,as}, K. Peters^{k,7}, J. Pettersson^{bn}, J.L. Ping^{ah}, R.G. Ping^{a,az}, A. Pitka^d, R. Poling^{bd}, V. Prasad^{bh,as}, H.R. Qi^b, M. Qi^{ai}, T.Y. Qi^b, S. Qian^{a,as}, C.F. Qiao^{az}, N. Qin^{bo}, X.P. Qin^m, X.S. Qin^d, Z.H. Qin^{a,as}, J.F. Qiu^a, S.Q. Qu^{aj}, K.H. Rashid^{bj,9}, K. Ravindran^u, C.F. Redmer^{ab}, M. Richter^d, A. Rivetti^{bm}, V. Rodin^{ae}, M. Rolo^{bm}, G. Rong^{a,az}, Ch. Rosner^o, M. Rump^{be}, A. Sarantsev^{ac,5}, M. Savrié^z, Y. Schelhaas^{ab}, K. Schoenning^{bn}, W. Shan^s, X.Y. Shan^{bh,as}, M. Shao^{bh,as}, C.P. Shen^b, P.X. Shen^{aj}, X.Y. Shen^{a,az}, H.Y. Sheng^a, X. Shi^{a,as}, X.D. Shi^{bh,as}, J.J. Song^{am}, Q.Q. Song^{bh,as}, X.Y. Song^a, S. Sosio^{bk,bm}, C. Sowa^d, S. Spataro^{bk,bm}, F.F. Sui^{am}, G.X. Sun^a, J.F. Sun^p, L. Sun^{bo}, S.S. Sun^{a,az}, X.H. Sun^a, Y.J. Sun^{bh,as}, Y.K. Sun^{bh,as}, Y.Z. Sun^a, Z.J. Sun^{a,as}, Z.T. Sun^a, Y.T. Tan^{bh,as}, C.J. Tang^{ap}, G.Y. Tang^a, X. Tang^a, V. Thoren^{bn}, B. Tsednee^{aa}, I. Uman^{ay}, B. Wang^a, B.L. Wang^{az}, C.W. Wang^{ai}, D.Y. Wang^{ak,12}, K. Wang^{a,as}, L.L. Wang^a, L.S. Wang^a, M. Wang^{am}, M.Z. Wang^{ak,12}, Meng Wang^{a,az}, P.L. Wang^a, R.M. Wang^{bp}, W.P. Wang^{bh,as}, X. Wang^{ak,12}, X.F. Wang^a, X.L. Wang^{i,10}, Y. Wang^{at}, Y. Wang^{bh,as}, Y.F. Wang^{a,as,az}, Y.Q. Wang^a, Z. Wang^{a,as}, Z.G. Wang^{a,as}, Z.Y. Wang^a, Zongyuan Wang^{a,az}, T. Weber^d, D.H. Wei^l, P. Weidenkaff^{ab}, F. Weidner^{be}, H.W. Wen^{ah}, S.P. Wen^a, U. Wiedner^d, G. Wilkinson^{bf}, M. Wolke^{bn}, L.H. Wu^a, L.J. Wu^{a,az}, Z. Wu^{a,as}, L. Xia^{bh,as}, Y. Xia^t, S.Y. Xiao^a, Y.J. Xiao^{a,az}, Z.J. Xiao^{ah}, Y.G. Xie^{a,as}, Y.H. Xie^f, T.Y. Xing^{a,az}, X.A. Xiong^{a,az}, Q.L. Xiu^{a,as}, G.F. Xu^a, J.J. Xu^{ai}, L. Xu^a, Q.J. Xuⁿ, W. Xu^{a,az}, X.P. Xu^{aq}, F. Yan^{bi}, L. Yan^{bk,bm}, W.B. Yan^{bh,as}, W.C. Yan^b, Y.H. Yan^t, H.J. Yang^{an,8}, H.X. Yang^a, L. Yang^{bo}, R.X. Yang^{bh,as}, S.L. Yang^{a,az}, Y.H. Yang^{ai}, Y.X. Yang^l, Yifan Yang^{a,az}, Z.Q. Yang^t, M. Ye^{a,as}, M.H. Ye^g, J.H. Yin^a, Z.Y. You^{at}, B.X. Yu^{a,as,az}, C.X. Yu^{aj}, J.S. Yu^t, T. Yu^{bi}, C.Z. Yuan^{a,az}, X.Q. Yuan^{ak,12}, Y. Yuan^a, A. Yuncu^{aw,1}, A.A. Zafar^{bj}, Y. Zeng^t, B.X. Zhang^a, B.Y. Zhang^{a,as}, C.C. Zhang^a, D.H. Zhang^a, H.H. Zhang^{at}, H.Y. Zhang^{a,as}, J. Zhang^{a,az}, J.L. Zhang^{bp}, J.Q. Zhang^d, J.W. Zhang^{a,as,az}, J.Y. Zhang^a, J.Z. Zhang^{a,az}, K. Zhang^{a,az}, L. Zhang^a, S.F. Zhang^{ai}, T.J. Zhang^{an,8}, X.Y. Zhang^{am}, Y. Zhang^{bh,as}, Y.H. Zhang^{a,as}, Y.T. Zhang^{bh,as}, Yang Zhang^a, Yao Zhang^a, Yi Zhang^{i,10}, Yu Zhang^{az}, Z.H. Zhang^f, Z.P. Zhang^{bh}, Z.Y. Zhang^{bo}, G. Zhao^a, J.W. Zhao^{a,as}, J.Y. Zhao^{a,az}, J.Z. Zhao^{a,as}, Lei Zhao^{bh,as}, Ling Zhao^a, M.G. Zhao^{aj}, Q. Zhao^a, S.J. Zhao^{br}, T.C. Zhao^a, Y.B. Zhao^{a,as}, Z.G. Zhao^{bh,as}, A. Zhemchugov^{ac,2}, B. Zheng^{bi}, J.P. Zheng^{a,as}, Y. Zheng^{ak,12}, Y.H. Zheng^{az}, B. Zhong^{ah}, L. Zhou^{a,as}, L.P. Zhou^{a,az}, Q. Zhou^{a,az}, X. Zhou^{bo}, X.K. Zhou^{az}, X.R. Zhou^{bh,as}, Xiaoyu Zhou^t, Xu Zhou^t, A.N. Zhu^{a,az}, J. Zhu^{aj}, J. Zhu^{at}, K. Zhu^a, K.J. Zhu^{a,as,az}, S.H. Zhu^{bg}, W.J. Zhu^{aj}, X.L. Zhu^{au}, Y.C. Zhu^{bh,as}, Y.S. Zhu^{a,az}, Z.A. Zhu^{a,az}, J. Zhuang^{a,as}, B.S. Zou^a, J.H. Zou^a

^a Institute of High Energy Physics, Beijing 100049, People's Republic of China

^b Beihang University, Beijing 100191, People's Republic of China

^c Beijing Institute of Petrochemical Technology, Beijing 102617, People's Republic of China

^d Bochum Ruhr-University, D-44780 Bochum, Germany

^e Carnegie Mellon University, Pittsburgh, PA 15213, USA

^f Central China Normal University, Wuhan 430079, People's Republic of China

^g China Center of Advanced Science and Technology, Beijing 100190, People's Republic of China

^h COMSATS University Islamabad, Lahore Campus, Defence Road, Off Raiwind Road, 54000 Lahore, Pakistan

ⁱ Fudan University, Shanghai 200443, People's Republic of China

^j G.I. Budker Institute of Nuclear Physics SB RAS (BINP), Novosibirsk 630090, Russia

^k GSI Helmholtzcentre for Heavy Ion Research GmbH, D-64291 Darmstadt, Germany

^l Guangxi Normal University, Guilin 541004, People's Republic of China

^m Guangxi University, Nanning 530004, People's Republic of China

ⁿ Hangzhou Normal University, Hangzhou 310036, People's Republic of China

^o Helmholtz Institute Mainz, Johann-Joachim-Becher-Weg 45, D-55099 Mainz, Germany

^p Henan Normal University, Xinxiang 453007, People's Republic of China

^q Henan University of Science and Technology, Luoyang 471003, People's Republic of China

^r Huangshan College, Huangshan 245000, People's Republic of China

^s Hunan Normal University, Changsha 410081, People's Republic of China

^t Hunan University, Changsha 410082, People's Republic of China

^u Indian Institute of Technology Madras, Chennai 600036, India

^v Indiana University, Bloomington, IN 47405, USA

^w INFN Laboratori Nazionali di Frascati, I-00044, Frascati, Italy

^x INFN and University of Perugia, I-06100, Perugia, Italy

^y INFN Sezione di Ferrara, I-44122, Ferrara, Italy
^z University of Ferrara, I-44122, Ferrara, Italy
^{aa} Institute of Physics and Technology, Peace Ave. 54B, Ulaanbaatar 13330, Mongolia
^{ab} Johannes Gutenberg University of Mainz, Johann-Joachim-Becher-Weg 45, D-55099 Mainz, Germany
^{ac} Joint Institute for Nuclear Research, 141980 Dubna, Moscow region, Russia
^{ad} Justus-Liebig-Universität Giessen, II. Physikalisches Institut, Heinrich-Buff-Ring 16, D-35392 Giessen, Germany
^{ae} KVI-CART, University of Groningen, NL-9747 AA Groningen, the Netherlands
^{af} Lanzhou University, Lanzhou 730000, People's Republic of China
^{ag} Liaoning University, Shenyang 110036, People's Republic of China
^{ah} Nanjing Normal University, Nanjing 210023, People's Republic of China
^{ai} Nanjing University, Nanjing 210093, People's Republic of China
^{aj} Nankai University, Tianjin 300071, People's Republic of China
^{ak} Peking University, Beijing 100871, People's Republic of China
^{al} Shandong Normal University, Jinan 250014, People's Republic of China
^{am} Shandong University, Jinan 250100, People's Republic of China
^{an} Shanghai Jiao Tong University, Shanghai 200240, People's Republic of China
^{ao} Shanxi University, Taiyuan 030006, People's Republic of China
^{ap} Sichuan University, Chengdu 610064, People's Republic of China
^{aq} Soochow University, Suzhou 215006, People's Republic of China
^{ar} Southeast University, Nanjing 211100, People's Republic of China
^{as} State Key Laboratory of Particle Detection and Electronics, Beijing 100049, Hefei 230026, People's Republic of China
^{at} Sun Yat-Sen University, Guangzhou 510275, People's Republic of China
^{au} Tsinghua University, Beijing 100084, People's Republic of China
^{av} Ankara University, 06100 Tandogan, Ankara, Turkey
^{aw} Istanbul Bilgi University, 34060 Eyup, Istanbul, Turkey
^{ax} Uludag University, 16059 Bursa, Turkey
^{ay} Near East University, Nicosia, North Cyprus, Mersin 10, Turkey
^{az} University of Chinese Academy of Sciences, Beijing 100049, People's Republic of China
^{ba} University of Hawaii, Honolulu, HI 96822, USA
^{bb} University of Jinan, Jinan 250022, People's Republic of China
^{bc} University of Manchester, Oxford Road, Manchester, M13 9PL, United Kingdom
^{bd} University of Minnesota, Minneapolis, MN 55455, USA
^{be} University of Muenster, Wilhelm-Klemm-Str. 9, 48149 Muenster, Germany
^{bf} University of Oxford, Keble Rd, Oxford, OX13RH, United Kingdom
^{bg} University of Science and Technology Liaoning, Anshan 114051, People's Republic of China
^{bh} University of Science and Technology of China, Hefei 230026, People's Republic of China
^{bi} University of South China, Hengyang 421001, People's Republic of China
^{bj} University of the Punjab, Lahore-54590, Pakistan
^{bk} University of Turin, I-10125, Turin, Italy
^{bl} University of Eastern Piedmont, I-15121, Alessandria, Italy
^{bm} INFN, I-10125, Turin, Italy
^{bn} Uppsala University, Box 516, SE-75120 Uppsala, Sweden
^{bo} Wuhan University, Wuhan 430072, People's Republic of China
^{bp} Xinyang Normal University, Xinyang 464000, People's Republic of China
^{bq} Zhejiang University, Hangzhou 310027, People's Republic of China
^{br} Zhengzhou University, Zhengzhou 450001, People's Republic of China

ARTICLE INFO

Article history:

Received 29 July 2019

Received in revised form 30 September 2019

Accepted 7 October 2019

Available online 10 October 2019

Editor: L. Rolandi

Keywords:

BESIII

D meson

Hadronic decays

Branching fractions

ABSTRACT

The four decay modes $D^0 \rightarrow \phi\pi^0$, $D^0 \rightarrow \phi\eta$, $D^+ \rightarrow \phi\pi^+$, and $D^+ \rightarrow \phi K^+$ are studied by using a data sample taken at the centre-of-mass energy $\sqrt{s} = 3.773$ GeV with the BESIII detector, corresponding to an integrated luminosity of 2.93 fb^{-1} . The branching fractions of the first three decay modes are measured to be $\mathcal{B}(D^0 \rightarrow \phi\pi^0) = (1.168 \pm 0.028 \pm 0.028) \times 10^{-3}$, $\mathcal{B}(D^0 \rightarrow \phi\eta) = (1.81 \pm 0.46 \pm 0.06) \times 10^{-4}$, and $\mathcal{B}(D^+ \rightarrow \phi\pi^+) = (5.70 \pm 0.05 \pm 0.13) \times 10^{-3}$, respectively, where the first uncertainties are statistical and the second are systematic. In addition, the upper limit of the branching fraction for $D^+ \rightarrow \phi K^+$ is given to be 2.1×10^{-5} at the 90% confidence level. The ratio of $\mathcal{B}(D^0 \rightarrow \phi\pi^0)$ to $\mathcal{B}(D^+ \rightarrow \phi\pi^+)$ is calculated to be $(20.49 \pm 0.50 \pm 0.45)\%$, which is consistent with the theoretical prediction based on isospin symmetry between these two decay modes.

© 2019 The Author(s). Published by Elsevier B.V. This is an open access article under the CC BY license (<http://creativecommons.org/licenses/by/4.0/>). Funded by SCOAP³.

* Corresponding authors.

E-mail addresses: houyingrui16@mails.ucas.ac.cn (Y.R. Hou), linchx5@mail2.sysu.edu.cn (C.X. Lin).

¹ Also at Bogazici University, 34342 Istanbul, Turkey.

² Also at the Moscow Institute of Physics and Technology, Moscow 141700, Russia.

³ Also at the Functional Electronics Laboratory, Tomsk State University, Tomsk, 634050, Russia.

⁴ Also at the Novosibirsk State University, Novosibirsk, 630090, Russia.

⁵ Also at the NRC "Kurchatov Institute", PNPI, 188300, Gatchina, Russia.

⁶ Also at Istanbul Arel University, 34295 Istanbul, Turkey.

⁷ Also at Goethe University Frankfurt, 60323 Frankfurt am Main, Germany.

⁸ Also at Key Laboratory for Particle Physics, Astrophysics and Cosmology, Ministry of Education; Shanghai Key Laboratory for Particle Physics and Cosmology; Institute of Nuclear and Particle Physics, Shanghai 200240, People's Republic of China.

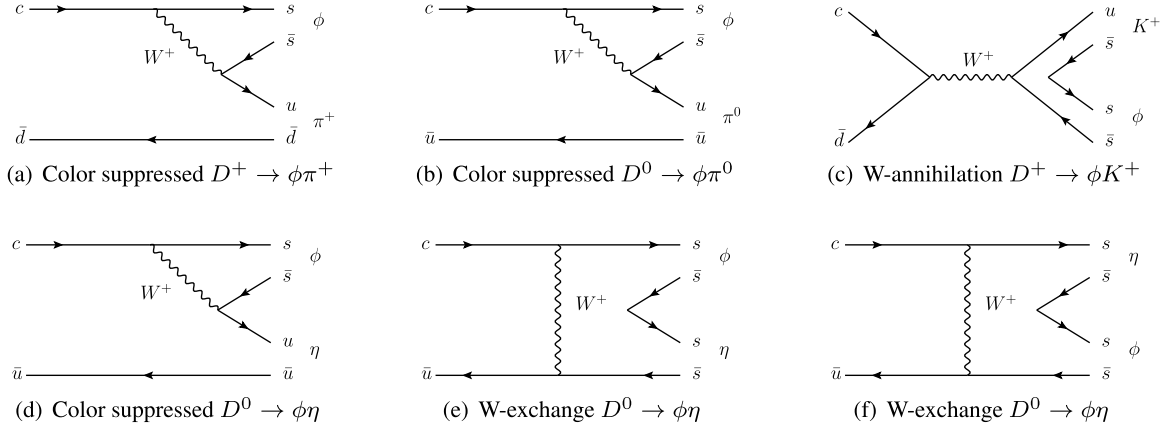


Fig. 1. Feynman diagrams of four $D \rightarrow \phi P$ decay modes.

Table 1

Current result of the ratio of $\mathcal{B}(D^0 \rightarrow \phi\pi^0)$ to $\mathcal{B}(D^+ \rightarrow \phi\pi^+)$.

The ratio	Experiment result (%)	Prediction (%)
$\frac{\mathcal{B}(D^0 \rightarrow \phi\pi^0)}{\mathcal{B}(D^+ \rightarrow \phi\pi^+)}$	24.6 ± 1.8 [5,6]	19.7 ± 0.2 [11]

1. Introduction

Comprehensive and precise measurements of hadronic D meson decays provide important inputs for the experimental studies of both charm and beauty decays [1]. One category of decay modes $D \rightarrow \phi P$ (P represents a pseudoscalar particle) has simple Feynman diagrams as depicted in Fig. 1. This facilitates theoretical predictions and their comparisons [2,3] to experimental measurements. However, the experimental measurements of $D \rightarrow \phi P$ are still limited [4] due to the relative low branching fractions (BF) which are suppressed by phase space due to the ϕ meson mass. The singly Cabibbo-suppressed (SCS) decays of $D^+ \rightarrow \phi\pi^+$ [5], $D^0 \rightarrow \phi\pi^0$ [6], and $D^0 \rightarrow \phi\eta$ [7] have been studied by CLEO, BaBar and Belle, respectively. The BF of the doubly Cabibbo-suppressed (DCS) decay $D^+ \rightarrow \phi K^+$ is derived out according to two measurements of the total BF for $D^+ \rightarrow K^- K^+ K^+$ and the intermediate fraction of ϕK^+ at LHCb [8,9].

According to isospin symmetry between u and d quarks, the BFs for $D^0 \rightarrow \phi\pi^0$ and $D^+ \rightarrow \phi\pi^+$ are connected [2,3] as follows:

$$\frac{\mathcal{B}(D^0 \rightarrow \phi\pi^0)}{\mathcal{B}(D^+ \rightarrow \phi\pi^+)} = \frac{1}{2} \frac{\Gamma_{D^+}}{\Gamma_{D^0}} = \frac{1}{2} \frac{\tau_{D^0}}{\tau_{D^+}}. \quad (1)$$

However, the current experimental result for the BF ratio deviates from prediction value of Eq. (1) by 2.7σ as shown in Table 1. Therefore, improved measurement is necessary to further test it and help to understand the strong interaction in D meson hadronic decays.

In this analysis, we study four two-body decay modes of $D \rightarrow \phi P$, which are $D^+ \rightarrow \phi K^+$, $D^+ \rightarrow \phi\pi^+$, $D^0 \rightarrow \phi\pi^0$, and $D^0 \rightarrow \phi\eta$, based on a data set of 2.93 fb^{-1} [10] taken at $\sqrt{s} = 3.773 \text{ GeV}$ with the BESIII detector. Due to energy conservation, the D and \bar{D} mesons from $e^+e^- \rightarrow \psi(3770) \rightarrow D\bar{D}$ are always produced in a

pair without any other accompanying hadrons. Throughout this paper, charge-conjugate modes are implied.

2. BESIII detector and Monte Carlo simulation

The BESIII detector is a magnetic spectrometer [12] located at the Beijing Electron Positron Collider (BEPCII) [13]. The cylindrical core of the BESIII detector consists of a helium-based multilayer drift chamber (MDC), a plastic scintillator time-of-flight system (TOF), and a CsI(Tl) electromagnetic calorimeter (EMC), which are all enclosed in a superconducting solenoidal magnet providing a 1.0 T magnetic field. The solenoid is supported by an octagonal flux-return yoke with resistive plate counter muon identifier modules interleaved with steel. The acceptance of charged particles and photons is 93% of the 4π solid angle. The charged-particle momentum resolution at 1 GeV/c is 0.5%, and the specific energy loss (dE/dx) resolution is 6% for electrons from Bhabha scattering. The EMC measures photon energies with a resolution of 2.5% (5%) at 1 GeV in the barrel (end cap) region. The time resolution of the TOF barrel section is 68 ps, while that of the end cap is 110 ps.

Simulated samples produced with the GEANT4-based [14] Monte Carlo (MC) package, which includes the geometric description [15, 16] of the BESIII detector and the detector response, are used to determine the detection efficiency and to estimate the backgrounds. The simulation includes the beam energy spread and initial state radiation (ISR) in the e^+e^- annihilations modelled with the generator KKMC [17]. The inclusive MC samples consist of the production of $D\bar{D}$ pairs, the non- $D\bar{D}$ decays of the $\psi(3770)$, the ISR production of the J/ψ and $\psi(3686)$ states, and the continuum processes incorporated in KKMC [17]. The equivalent luminosity of the inclusive MC samples is about 10 times that of the data. The known decay modes are modelled with EVTGEN [18] using branching fractions taken from the Particle Data Group [4], and the remaining unknown decays from the charmonium states with LUNDCHARM [19]. The final state radiations (FSR) from charged final state particles are incorporated with the PHOTOS (version 2.02) package [20,21]. The signal processes are generated separately taking the spin-matrix elements into account in EVTGEN. For each signal channel, 200 000 events are simulated.

3. Event selection

Candidates of the decay modes $D \rightarrow \phi P$ are reconstructed by combining the final states of K^\pm , π^\pm , π^0 , and η particles with BESIII offline software system [1,22], where ϕ mesons are detected via decays to K^+K^- . Candidates for π^0 and η are identified from $\pi^0 \rightarrow \gamma\gamma$ and $\eta \rightarrow \gamma\gamma$, respectively.

⁹ Also at Government College Women University, Sialkot - 51310, Punjab, Pakistan.

¹⁰ Also at Key Laboratory of Nuclear Physics and Ion-beam Application (MOE) and Institute of Modern Physics, Fudan University, Shanghai 200443, People's Republic of China.

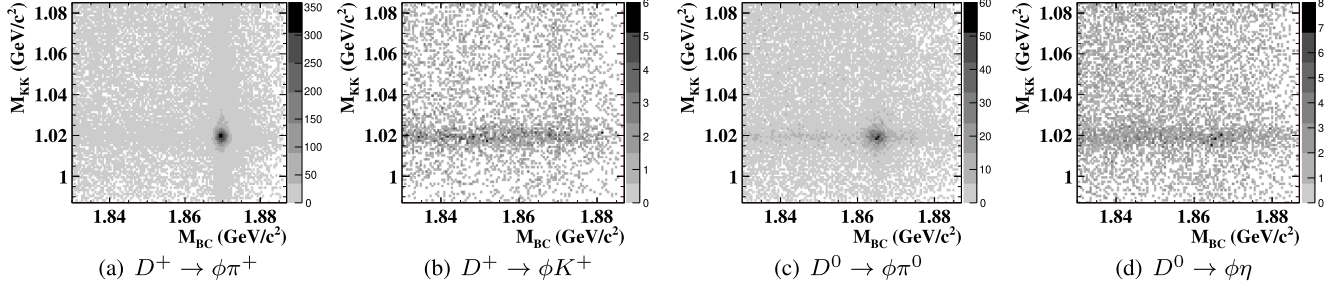
¹¹ Also at Harvard University, Department of Physics, Cambridge, MA, 02138, USA.

¹² Also at State Key Laboratory of Nuclear Physics and Technology, Peking University, Beijing 100871, People's Republic of China.

Table 2

For each signal mode, the requirement on ΔE , signal yields N_{sig}^i , MC-determined detection efficiency ε^i , branching fraction \mathcal{B}^i in this work, and the corresponding world results \mathcal{B}_{ext} .

Decay mode	ΔE (GeV)	N_{sig}^i	ε^i (%)	$\mathcal{B}^i (\times 10^{-4})$	$\mathcal{B}_{\text{ext}} (\times 10^{-4})$
$D^+ \rightarrow \phi\pi^+$	$[-0.020, 0.019]$	17527 ± 152	37.7 ± 0.1	$57.0 \pm 0.5 \pm 1.3$	53.7 ± 2.3 [4]
$D^+ \rightarrow \phi K^+$	$[-0.019, 0.018]$	12_{-12}^{+28}	23.7 ± 0.1	$0.062_{-0.062}^{+0.144} \pm 0.002$ < 0.21 at 90% CL	0.085 ± 0.011 [4,8,9]
$D^0 \rightarrow \phi\pi^0$	$[-0.077, 0.035]$	3333 ± 76	27.7 ± 0.1	$11.68 \pm 0.28 \pm 0.28$	13.2 ± 0.8 [4]
$D^0 \rightarrow \phi\eta$	$[-0.040, 0.038]$	102 ± 26	13.7 ± 0.1	$1.81 \pm 0.46 \pm 0.06$	1.4 ± 0.5 [4]

**Fig. 2.** Two-dimensional distributions of M_{BC} and M_{KK} in data for the four signal modes.

Selected charged tracks must satisfy $|\cos\theta| < 0.93$, where θ is the polar angle with respect to the beam axis. The distance of closest approach of the track to the interaction point is required to be less than 10 cm in the beam direction and less than 1 cm in the plane perpendicular to the beam. Separation of charged kaons from charged pions is implemented by combining the energy loss (dE/dx) in the MDC and the time-of-flight information from the TOF. We calculate the probabilities $P(K)$ and $P(\pi)$ with the hypothesis of K or π , and require that K candidates have $P(K) > P(\pi)$, while π candidates have $P(\pi) > P(K)$.

Photon candidates are selected from neutral showers deposited in the EMC crystals, with energies larger than 25 MeV in the barrel ($|\cos\theta| < 0.8$) and 50 MeV in the end cap ($0.86 < |\cos\theta| < 0.92$). To reduce fake photons due to beam background or electronic noise, the shower clusters are required to be within $[0, 700]$ ns from the event start time. Furthermore, the photon candidates are required to be at least 10° away from any charged tracks to remove fake photons caused by the interactions of hadrons in the EMC.

The $\pi^0(\eta)$ candidates are formed with pairs of photon candidates, whose invariant mass, $M_{\gamma\gamma}$, is required to be within $[0.115, 0.150]$ ($[0.500, 0.560]$) GeV/c^2 . To improve momentum resolution, a 1C kinematic fit constraining the reconstructed $\pi^0(\eta)$ mass to the nominal mass [4] is performed and the fitted four-momentum of the $\pi^0(\eta)$ is used in further analysis.

4. Data analysis

In the rest frame of the initial e^+e^- system, the total collision energy is shared equally by the $D\bar{D}$ pair. Hence, in this frame two variables, the energy difference ΔE and the beam constrained mass M_{BC} related to energy and momentum conservation, respectively, are defined as

$$\Delta E \equiv E_D - \sqrt{s}/2,$$

$$M_{\text{BC}} \equiv \sqrt{s/4c^4 - |\vec{p}_D|^2/c^2},$$

where \vec{p}_D is the momentum of the D candidate.

Signals for the four ϕP decay modes are expected to peak around zero in ΔE distributions and the D nominal mass in M_{BC}

distributions. To suppress combinatorial background, the ΔE of the D candidates are required to be within the regions listed in Table 2 for the different signal modes, which correspond to about 3σ coverage. The asymmetric boundaries of the ΔE region for the $\phi\pi^0$ and $\phi\eta$ modes are due to energy leakage in the EMC when reconstructing the photon energy. If there is more than one D candidate left for one signal decay mode in an event, the candidate with the smallest $|\Delta E|$ is chosen for further analysis. More than 60% of events have multiple candidates for D^0 decay modes and 20% for D^+ decay modes. According to the studies on MC samples, the probability to select the correct candidate by choosing the minimum $|\Delta E|$ is more than 90%. In addition, the credibility of this method is verified and proven to be robust by studying the high-statistics inclusive MC samples.

As shown in Fig. 2 and Fig. 3, clear peaks are seen in the M_{BC} and M_{KK} distributions for the four signal modes, which correspond to the $D \rightarrow K^+K^-P$ signals and $\phi \rightarrow K^+K^-$ signals, respectively. According to the studies based on the inclusive MC samples, three types of background events will pass through above selection criteria. The first one is a true D meson decaying to K^+K^-P final states without a ϕ meson involved ($D \rightarrow K^+K^-P$), the second one is a true ϕ meson not from the corresponding signal mode (Cont. ϕPX) and the third one is the combinatorial background from neither of the previous two sources (Comb. bkg).

Two-dimensional unbinned extended maximum likelihood fits to the obtained distributions of M_{BC} and M_{KK} are performed to extract yields of signals, as shown in Fig. 3. The M_{KK} variable is employed here to discriminate the ϕ meson signal from the non-resonant K^+K^- final state. The probability density functions of the D meson and ϕ meson signals are modeled by the MC-simulated signal shapes convoluted with Gaussian functions that describe the resolution differences between MC simulations and data. The combinatorial backgrounds in M_{BC} (M_{KK}) are described with (inverted) ARGUS [23] functions based on the studies on the inclusive MC sample. Since the correlation between M_{KK} and M_{BC} can be neglected, these two variables are considered uncorrelated in the fit. The parameters of the (inverted) ARGUS and Gaussian functions in two-dimensional fits are fixed according to one-dimensional fits to the corresponding M_{BC} and M_{KK} distributions. The obtained signal yields are given in Table 2.

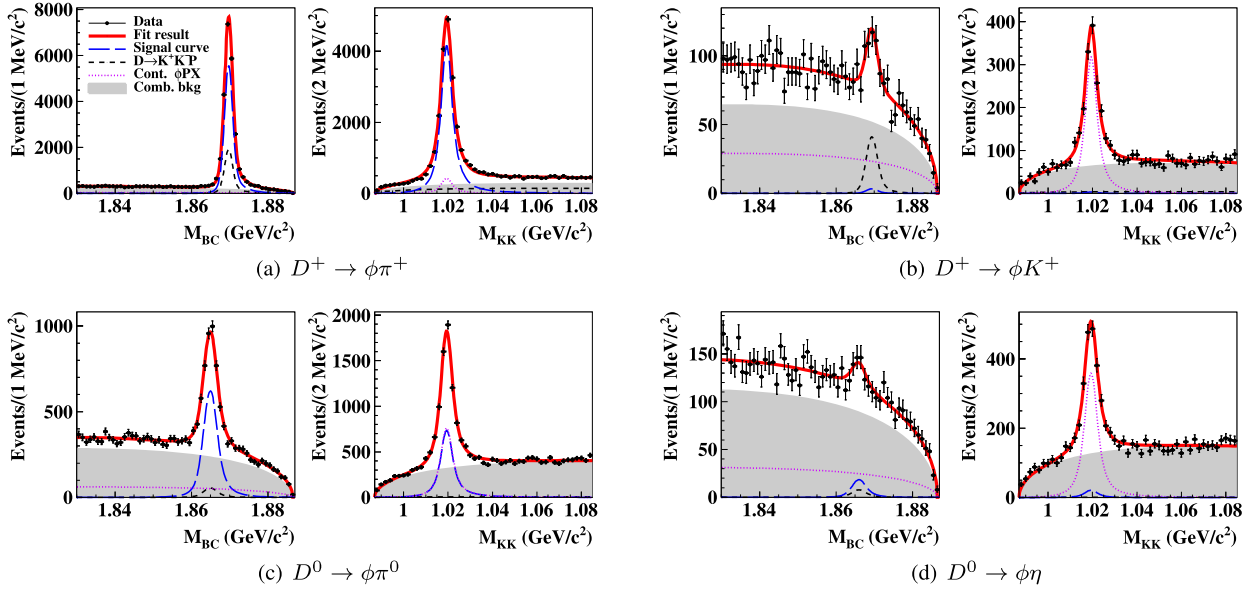


Fig. 3. Two-dimensional unbinned maximum likelihood fits to the distributions of M_{BC} and M_{KK} in data for the four signal modes. The points with error bars are data, the (red) thick curves are the total fits, the (blue) long dashed curves describe the signals, the (violet) dotted curves represent backgrounds of true ϕ mesons not from $D \rightarrow \phi P$ decay modes, the (black) dashed curves describe backgrounds from $D \rightarrow K^+ K^- P$ without a ϕ meson, and the shaded area show the combinatorial backgrounds.

5. Branching fraction

The branching fractions for the $D \rightarrow \phi P$ decays can be calculated by

$$\mathcal{B}^i = \frac{N_{\text{sig}}^i}{2 \cdot N_{D\bar{D}} \cdot \varepsilon^i \cdot \mathcal{B}_{\text{sub}}^i}, \quad (2)$$

where i denotes a signal mode of $D \rightarrow \phi P$, N_{sig}^i is the signal yield extracted in data, $N_{D\bar{D}}$ is the number of $D\bar{D}$ event in data, which is $(8296 \pm 31 \pm 64) \times 10^3$ for $D^+ D^-$ and $(10597 \pm 28 \pm 89) \times 10^3$ for $D^0 \bar{D}^0$ [24] in the data set we analyzed, ε^i is the reconstruction efficiency determined from MC simulation of the signal mode, and $\mathcal{B}_{\text{sub}}^i$ are the branching fractions of the intermediate decay processes $\phi \rightarrow K^+ K^-$ and $\pi^0/\eta \rightarrow \gamma\gamma$, quoted from PDG [4]. The branching fraction for each decay mode is calculated in Table 2.

The statistical significance of the $D^0 \rightarrow \phi\eta$ signal is evaluated, taken as $\sqrt{-2\ln(\mathcal{L}_0^{\text{stat}}/\mathcal{L}_{\text{max}}^{\text{stat}})}$ where $\mathcal{L}_{\text{max}}^{\text{stat}}$ and $\mathcal{L}_0^{\text{stat}}$ are the maximum likelihood values with and without signal, respectively, to be 4.2σ . Since the significance of the observed $D^+ \rightarrow \phi K^+$ signal is 0.8σ , the upper limit of $\mathcal{B}(D^+ \rightarrow \phi K^+)$ is estimated by a likelihood scan method, which takes into account the systematic uncertainties as follows

$$\mathcal{L}_i(\mathcal{B}^i) = \int_{-1}^1 \mathcal{L}^{\text{stat}}[(1 + \Delta)\mathcal{B}^i] \exp\left(-\frac{\Delta^2}{2\sigma_{i,\text{syst}}^2}\right) d\Delta. \quad (3)$$

Here, Δ is the relative deviation of the estimated branching fraction from the nominal value and $\sigma_{i,\text{syst}}$ is the total systematic uncertainty given in Table 3.

The likelihood curve calculated according to Eq. (3) is shown in Fig. 4. The upper limit on $\mathcal{B}(D^+ \rightarrow \phi K^+)$ at the 90% confidence level (CL) is estimated to be 2.1×10^{-5} by integrating the likelihood curve in the physical region, $\mathcal{B}^i > 0$.

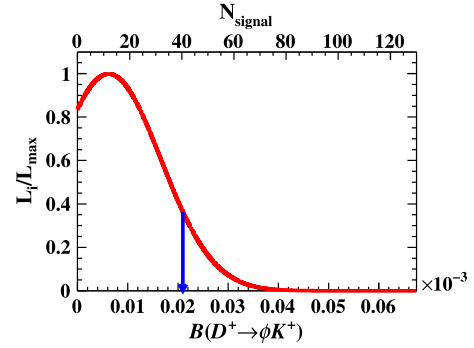


Fig. 4. Likelihood curve as the function of assumed $\mathcal{B}(D^+ \rightarrow \phi K^+)$. The arrow points to the position of upper limit at the 90% CL.

6. Systematic uncertainties

The following sources of systematic uncertainties, as given in Table 3, are considered. The total systematic uncertainty is determined by adding all contributions in quadrature.

The uncertainties of tracking and particle identification (PID) for charged kaon and pion mesons, as well as $\pi^0(\eta)$ reconstruction, have been studied in previous works by using control samples of D hadronic events [25]. The uncertainties are weighted according to the kinematics of the candidates. Furthermore, in order to estimate the systematic uncertainty caused by the selected $\pi^0(\eta)$ signal regions, the requirements on $M_{\gamma\gamma}$ are varied and the resultant changes on the BF's are 0.7% (1.1%). This uncertainty is combined with that of $\pi^0(\eta)$ reconstruction, the quadrature sum of which is given as 1.2% (1.8%). Requirements on ΔE are studied by smearing the corresponding ΔE distribution in inclusive MC samples with Gaussian functions and re-calculating detection efficiencies. The changes of the efficiencies are assigned as the corresponding uncertainties.

Systematic uncertainty related to the two-dimensional fit includes parameters of Gaussian and ARGUS functions, fit range and background models. For the fixed parameters in the Gaussian and ARGUS functions, their values are varied by $\pm 1\sigma$ from the one-

Table 3
Summary of systematic uncertainties in percentage.

Source	$D^+ \rightarrow \phi\pi^+$	$D^+ \rightarrow \phi K^+$	$D^0 \rightarrow \phi\pi^0$	$D^0 \rightarrow \phi\eta$	$\frac{\mathcal{B}(D^0 \rightarrow \phi\pi^0)}{\mathcal{B}(D^+ \rightarrow \phi\pi^+)}$
Tracking	1.0	1.1	0.8	1.0	0.3
PID	1.2	1.0	0.6	0.6	0.4
π^0 reconstruction	—	—	1.2	—	1.2
η reconstruction	—	—	—	1.8	—
ΔE requirement	0.2	0.2	0.2	0.2	0.3
2D fit	0.4	2.5	0.4	2.0	0.6
$N_{D\bar{D}}$ uncertainty	0.9	0.9	0.9	0.9	1.3
$\mathcal{B}(\phi \rightarrow K^+K^-)$	1.0	1.0	1.0	1.0	—
$\mathcal{B}(\pi^0, \eta \rightarrow \gamma\gamma)$	—	—	0.1	0.5	0.1
QC effect	—	—	1.0	1.0	1.0
Total	2.2	3.3	2.4	3.5	2.2

dimensional fit results and the largest resultant change is assigned as the systematic uncertainty. The uncertainty due to the fit range is estimated by repeating the fits with a series of varied ranges and the corresponding changes are found to be negligible. For the background models, potential background of $D \rightarrow f_0(980)P$ is included in the fit and the change on the number of signal events is assigned as uncertainty. This uncertainty is larger for $\mathcal{B}(D^+ \rightarrow \phi K^+)$ and $\mathcal{B}(D^0 \rightarrow \phi\eta)$ due to the smaller signal yields.

The uncertainties of the quoted $N_{D\bar{D}}$ from Ref. [24], $\mathcal{B}(\phi \rightarrow K^+K^-)$ and $\mathcal{B}(\pi^0/\eta \rightarrow \gamma\gamma)$ from PDG [4] are taken into account for the relevant signal modes. Since D^0 and \bar{D}^0 are coherently produced in the process $e^+e^- \rightarrow \psi(3770) \rightarrow D^0\bar{D}^0$, quantum coherence (QC) [26] should be considered according to the equation

$$\Delta N_{CP}^{obs} = y_{CP} \cdot N_{CP}^{obs}.$$

The uncertainty depends on the $D^0 - \bar{D}^0$ mixing parameter y_{CP} , and is taken to be 1.0% [27] conservatively.

For the systematic uncertainties of $\frac{\mathcal{B}(D^0 \rightarrow \phi\pi^0)}{\mathcal{B}(D^+ \rightarrow \phi\pi^+)}$, the effects related to K^\pm tracking and PID are mostly cancelled, owing to their same kinematic phase space. The remaining systematic uncertainties in Table 3 are considered independently and summed up in quadrature.

7. Summary

The decays of $D^+ \rightarrow \phi\pi^+$, $D^0 \rightarrow \phi\pi^0$, $D^0 \rightarrow \phi\eta$, and $D^+ \rightarrow \phi K^+$ are studied by analyzing 2.93 fb^{-1} data taken at $\sqrt{s} = 3.773 \text{ GeV}$ with the BESIII detector. The obtained BF's are consistent with previous results, as listed in Table 2, while the precisions of the BF's for the first three modes are improved. In addition, the upper limit on $\mathcal{B}(D^+ \rightarrow \phi K^+)$ of 2.1×10^{-5} at 90% CL is reported.

Our results of $\mathcal{B}(D \rightarrow \phi\pi)$ and $\mathcal{B}(D^0 \rightarrow \phi\eta)$ are consistent with the previous measurements. Furthermore, the ratio of $\mathcal{B}(D^0 \rightarrow \phi\pi^0)$ to $\mathcal{B}(D^+ \rightarrow \phi\pi^+)$ is calculated to be $(20.49 \pm 0.50 \pm 0.45)\%$, which is smaller than the previous result $(24.6 \pm 1.8)\%$ [5,6]. Meanwhile, the deviation from the predicted value of $(19.7 \pm 0.2)\%$ in Eq. (1) is reduced from 2.7σ to 1.2σ , which shows better agreement than the previous measurement. Hence, our results support the isospin symmetry between these two D meson decay modes.

Acknowledgements

The BESIII collaboration thanks the staff of BEPCII and the IHEP computing center for their strong support. This work is sup-

ported in part by National Key Basic Research Program of China under Contract No. 2015CB856700; National Natural Science Foundation of China (NSFC) under Contracts Nos. 11625523, 11635010, 11735014, 11822506, 11835012; the Chinese Academy of Sciences (CAS) Large-Scale Scientific Facility Program; Joint Large-Scale Scientific Facility Funds of the NSFC and CAS under Contracts Nos. U1532257, U1532258, U1732263, U1832207, U1932101; CAS Key Research Program of Frontier Sciences under Contracts Nos. QYZDJ-SSW-SLH003, QYZDJ-SSW-SLH040; 100 Talents Program of CAS; INPAC and Shanghai Key Laboratory for Particle Physics and Cosmology; ERC under Contract No. 758462; German Research Foundation DFG under Contracts Nos. Collaborative Research Center CRC 1044, FOR 2359; Istituto Nazionale di Fisica Nucleare, Italy; Koninklijke Nederlandse Akademie van Wetenschappen (KNAW) under Contract No. 530-4CDP03; Ministry of Development of Turkey under Contract No. DPT2006K-120470; National Science and Technology fund; STFC (United Kingdom); The Knut and Alice Wallenberg Foundation (Sweden) under Contract No. 2016.0157; The Royal Society, UK under Contracts Nos. DH140054, DH160214; The Swedish Research Council; U.S. Department of Energy under Contracts Nos. DE-FG02-05ER41374, DE-SC-0010118, DE-SC-0012069; University of Groningen (RuG) and the Helmholtzzentrum fuer Schwerionenforschung GmbH (GSI), Darmstadt.

References

- [1] D.M. Asner, et al., Int. J. Mod. Phys. A 24 (2009) S1.
- [2] Q. Qin, H.N. Li, C.D. Lv, F.S. Yu, Phys. Rev. D 89 (2014) 054006.
- [3] H.Y. Cheng, C.W. Chiang, Phys. Rev. D 81 (2010) 071021.
- [4] M. Tanabashi, et al., Particle Data Group, Phys. Rev. D 98 (2018) 030001.
- [5] P. Rubin, et al., CLEO Collaboration, Phys. Rev. D 78 (2008) 072003.
- [6] B. Aubert, et al., BaBar Collaboration, Phys. Rev. D 76 (2007) 011102.
- [7] K. Abe, et al., Belle Collaboration, Phys. Rev. Lett. 92 (2004) 101803.
- [8] R. Aaij, et al., LHCb Collaboration, J. High Energy Phys. 04 (2019) 63.
- [9] R. Aaij, et al., LHCb Collaboration, J. High Energy Phys. 03 (2019) 176.
- [10] M. Ablikim, et al., BESIII Collaboration, Chin. Phys. C 37 (2013) 123001; Phys. Lett. B 753 (2016) 629.
- [11] J.M. Link, et al., FOCUS Collaboration, Phys. Lett. B 537 (2002) 192.
- [12] M. Ablikim, et al., BESIII Collaboration, Nucl. Instrum. Methods A 614 (2010) 345.
- [13] C.H. Yu, et al., in: Proceedings of IPAC2016, Busan, Korea, 2016.
- [14] S. Agostinelli, et al., GEANT4 Collaboration, Nucl. Instrum. Methods A 506 (2003) 250.
- [15] Y. Liang, B. Zhu, Z. You, et al., Nucl. Instrum. Methods A 603 (2009) 325.
- [16] Z.Y. You, Y.T. Liang, Y.J. Mao, Chin. Phys. C 32 (2008) 572.
- [17] S. Jadach, B.F.L. Ward, Z. Was, Phys. Rev. D 63 (2001) 113009; S. Jadach, B.F.L. Ward, Z. Was, Comput. Phys. Commun. 130 (2000) 260.
- [18] D.J. Lange, Nucl. Instrum. Methods A 462 (2001) 152; R.G. Ping, Chin. Phys. C 32 (2008) 599.
- [19] J.C. Chen, G.S. Huang, X.R. Qi, D.H. Zhang, Y.S. Zhu, Phys. Rev. D 62 (2000) 034003; R.L. Yang, R.G. Ping, H. Chen, Chin. Phys. Lett. 31 (2014) 061301.
- [20] E. Richter-Was, Phys. Lett. B 303 (1993) 163.

- [21] P. Golonka, Z. Was, Eur. Phys. J. C 45 (2006) 97.
- [22] W. Li, et al., in: Proc. Int. Conf. Comput. High Energy and Nucl. Phys., 2006, p. 225.
- [23] H. Albrecht, et al., ARGUS Collaboration, Phys. Lett. B 241 (1990) 278.
- [24] M. Ablikim, et al., BESIII Collaboration, Chin. Phys. C 42 (2018) 083001.
- [25] M. Ablikim, et al., BESIII Collaboration, Phys. Rev. D 97 (2018) 072004.
- [26] D. Asner, W. Sun, Phys. Rev. D 73 (2006) 034024;
D. Asner, W. Sun, Phys. Rev. E 77 (2008) 019901.
- [27] Y. Amhis, et al., Heavy Flavor Averaging Group, Eur. Phys. J. C 77 (2017) 895.